Biomaterials

International Edition: DOI: 10.1002/anie.201507352
German Edition: DOI: 10.1002/ange.201507352

Magnesium Corrosion Triggered Spontaneous Generation of H_2O_2 on Oxidized Titanium for Promoting Angiogenesis

*Jimin Park, Ping Du, Jin-Kyung Jeon, Gun Hyuk Jang, Mintai Peter Hwang, Hyung-Seop Han, Kwideok Park, Kwan Hyi Lee, Jee-Wook Lee, Hojeong Jeon, Yu-Chan Kim, Jong Woong Park, Hyun-Kwang Seok, and Myoung-Ryul Ok**

Abstract: *Although the use of reactive oxygen species (ROS) has been extensively studied, current systems employ external stimuli such as light or electrical energy to produce ROS, which limits their practical usage. In this report, biocompatible metals were used to construct a novel electrochemical system that can spontaneously generate H_2O_2 without any external light or voltage. The corrosion of Mg transfers electrons to Au-decorated oxidized Ti in an energetically favorable process, and the spontaneous generation of H_2O_2 in an oxygen reduction reaction was revealed to occur at titanium by combined spectroscopic and electrochemical analyses. The controlled release of H_2O_2 noticeably enhanced in vitro angiogenesis even in the absence of growth factors. Finally, a new titanium implant prototype was developed by Mg incorporation, and its potential for promoting angiogenesis was demonstrated.*

Reactive oxygen species (ROS) play pivotal roles in numerous physiological processes in vivo, and their unique redox properties have served as a basis for the development of a number of biological breakthroughs.[1–4] Not surprisingly, interest in the generation of ROS has increased, underscored by emerging studies demonstrating artificial ROS formation.[4–6] In particular, ROS photogenerated from metal oxides have been shown to exert an oxidative stress on cells and have been utilized accordingly in anticancer and antibacterial applications.[6,7] Interestingly, lower levels of ROS regulate cellular redox signaling without exerting their cytotoxic effects, and have been shown to thereby promote physiological events such as cell migration and proliferation.[6–9] Among the various ROS species, hydrogen peroxide (H_2O_2) has been implicated as an important species in redox signaling during angiogenesis, and H_2O_2 released from metal oxides has been shown to promote angiogenesis in both in vitro and in vivo models.[2,7–9] However, the application of photogenerated ROS is limited by the difficulties associated with delivering light into a physiological environment.

In another approach, electrochemical systems comprising a metal oxide as the cathode and a noble metal as the counterelectrode have been investigated for generating ROS.[10–12] However, the introduction of an external potential source confers further complexity and thus hinders biological applications. Put together, a crucial limitation of current systems is that an external stimulus such as light or electrical energy is required for the formation of ROS, thereby thwarting their practical use in physiological environments. Moreover, as ROS exert concentration-dependent effects on cells,[2–3] controlling the amount of ROS in an application-specific manner is pivotal. In this regard, a system that can generate ROS in a controlled manner in the absence of external stimuli is highly desirable for potential biological applications.

The corrosion of biocompatible metals can be an alternative and simple electron source to metal oxides for generating ROS. When the Fermi level of the metal is higher than the conduction band of the oxide, the electrons generated by corrosion of the metal can be transferred into the conduction band in an energetically favorable way (Scheme 1 a). The reducing power of the transferred electrons is sufficient for oxygen reduction, and ROS can thus be generated by metal corrosion triggered electron transfer. Among various biocompatible metals, magnesium is a promising candidate owing to its high reducing power and excellent biodegradability.[13–15]

Herein, we have developed a novel electrochemical system that can spontaneously generate H_2O_2 through the corrosion of a biocompatible metal. Inspired by the high biocompatibility of Mg and Ti,[13–16] which are both used in orthopedic implants, we used Mg- and Au-decorated oxidized Ti as the anode and cathode parts, respectively (Scheme 1 b). Oxidized Ti was chosen as the cathode material because of its facile formation on Ti metal by anodization and its proven catalytic ability in the oxygen reduction reaction (ORR).[10–12] Our system generated H_2O_2 in phosphate buffered saline (PBS) and cell-culture media in a controlled manner, as determined by combined spectroscopic and electrochemical

[*] J. Park, Dr. P. Du, J.-K. Jeon, G. H. Jang, M. P. Hwang, H.-S. Han, Dr. K. Park, Dr. K. H. Lee, Dr. H. Jeon, Dr. Y.-C. Kim, Dr. H.-K. Seok, Dr. M.-R. Ok
Center for Biomaterials
Korea Institute of Science & Technology
Seoul 136-650 (South Korea)
E-mail: omr2da@kist.re.kr

J.-K. Jeon, Dr. K. Park, Dr. K. H. Lee, Dr. H. Jeon, Dr. Y.-C. Kim, Dr. H.-K. Seok
Korea University of Science and Technology
Daejeon 34113 (South Korea)

Dr. J.-W. Lee
School of Advanced Materials Engineering, Kookmin University
Seoul 136-702 (South Korea)

M. D. J. W. Park
Department of Orthopedic Surgery
School of Medicine, Korea University
Seoul (South Korea)

Supporting information for this article is available on the WWW under http://dx.doi.org/10.1002/anie.201507352.

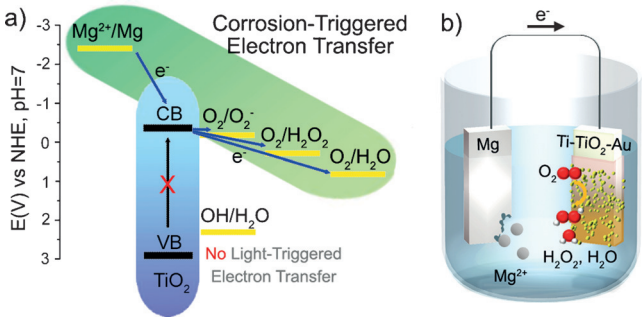

Scheme 1. a) Fermi level of Mg, energy bands of TiO_2, and redox potentials of O_2/O_2^-, O_2/H_2O_2, and O_2/H_2O. Electrons from Mg can be transferred into the conduction band of TiO_2 where an oxygen reduction reaction occurs through an energetically favorable pathway. b) Schematic representation of the Mg and Ti/TiO_2/Au based electrochemical cell. In the anode, Mg corrodes into Mg^{2+} ions, thereby generating electrons that reduce O_2 molecules at the cathode without an additional applied voltage.

techniques. By controlling the amount of H_2O_2 released, we demonstrated that our system can be used for promoting angiogenesis in vitro. Moreover, we developed an implant prototype that consists of a Mg anode inside oxidized Ti metal, and demonstrated its potential for promoting angiogenesis.

A TiO_2 layer was formed on a Ti substrate according to a facile, previously described anodizing method.[17] Au clusters were then deposited onto the TiO_2 layer to improve the catalytic ability of TiO_2 in the ORR.[10,12] A cross-section of the Ti/TiO_2/Au cathode was obtained by cutting with a focused ion beam (FIB) and examined by transmission electron microscopy (TEM) analysis (Figure 1 a–c). At the topmost surface of the cathode, approximately 3 nm sized Au clusters were well-distributed over the amorphous TiO_2 films with a thickness of about 20 nm (Figure 1 a). A closer examination of these regions by HR-TEM indicated Au cluster lattice spacings of 0.230 nm and 0.205 nm, which are in good agreement with the inter-plane distances of Au{111} and Au{200}, respectively (Figure 1 b). Whereas the anodized TiO_2 layer did not display any noticeable crystallinity or atomic arrangement, the Ti substrate was highly crystalline and comprised (001) and (101) planes (Figure 1 b). Point energy-dispersive X-ray (EDX) analysis confirmed that the well-ordered structures comprise three layers (Figures 1 c; see also the Supporting Information, Figure S1). Moreover, X-ray photoelectron spectroscopy (XPS) and atomic force microscopy (AFM) measurements showed that clusters of approximately 3 nm height had been deposited onto the substrate and clearly revealed the Au 4d and 4f peaks (Figure 1 d, e and S2).

The electrochemical characteristics of the Mg-Ti/TiO_2/Au system were evaluated at pH 7.4 in PBS in the presence and absence of O_2 at 37 °C. The voltages of Mg vs. Ag/AgCl, Ti/TiO_2/Au vs. Ag/AgCl, and Ti/TiO_2/Au vs. Mg were recorded as a function of the discharging current density in the O_2-saturated PBS solution (Figure S3 a). For a discharging current of up to 1.0 mA cm^{-2}, the voltage of Mg vs. Ag/AgCl was maintained around −1.5 V. This voltage is in good agreement with that given in previous report, which showed that the dominant anodic reaction is corrosion of Mg into Mg^{2+} ions or $Mg(OH)_2$.[18] Indeed, optical and scanning electron microscopy (SEM), TEM, selected-area electron diffraction (SAED) analysis, and EDX spectroscopy showed that white precipitates, that is, crystalline $Mg(OH)_2$, had formed on the Mg surface after the discharging tests in solution (Figure S4–S8).

Contrary to the voltage at the Mg anode, that of Ti/TiO_2/Au vs. Ag/AgCl gradually decreased from −0.2 V to −1.2 V as the discharging current density increased from 0 to 1.0 mA cm^{-2}, and a sharp decrease in the voltage was observed at a current density of approximately 0.6 mA cm^{-2} (Figure S3 a). The change in the voltage with the current density indicates that the nature of the cathodic reaction depends on the current density.[18] Several reduction processes are possible at −0.2 V to −1.2 V vs. Ag/AgCl: oxygen reduction to H_2O_2 or H_2O (0.065 V and 0.59 V vs. Ag/AgCl) or hydrogen evolution (−0.64 V vs. Ag/AgCl) at pH 7.4. Based on the theoretical reduction potentials of the three reactions, the ORR is dominant at lower discharging currents whereas hydrogen evolution dominates at higher currents. Owing to the decrease in the Ti/TiO_2/Au vs. Ag/AgCl voltage with the discharging current, the overall voltage of Ti/TiO_2/Au vs. Mg consequently decreases with an increase in the discharging current (Figure S3 a).

The occurrence of the ORR at the cathode was confirmed by control experiments in N_2-saturated PBS solution (Figure S3 b). Contrary to the voltage of Ti/TiO_2/Au vs. Ag/AgCl in O_2-saturated conditions, which decreased sharply to −1.0 V at a discharging current density of approx-

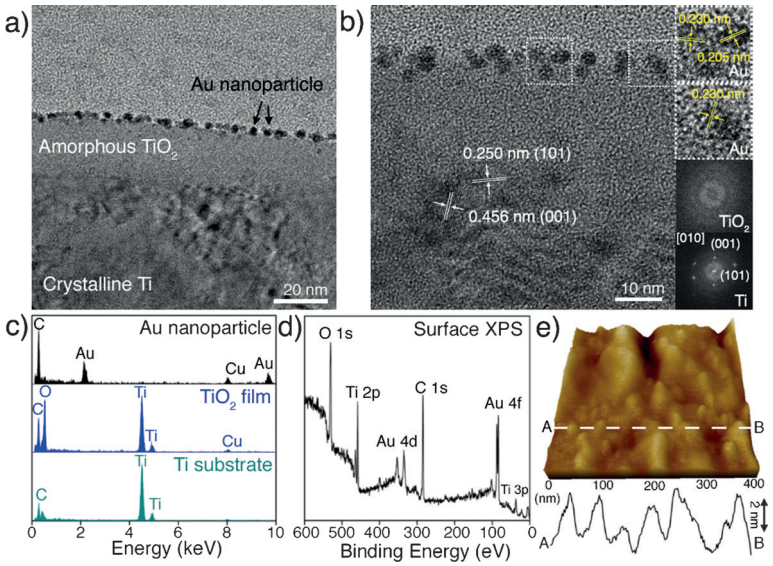

Figure 1. a) TEM images of the cross-section of a Ti/TiO_2/Au plate cut with a focused ion beam (FIB). b) HR-TEM images and FFTs of the three regions. Lattice fringes in the Ti and Au regions are indicated by white and yellow arrows, respectively. c) Point EDX spectrum for the Au, TiO_2, and Ti regions. The Cu peak is a result of the Cu TEM grid. d) XPS spectra and e) AFM images of the Ti/TiO_2/Au surface.

imately 0.6 mA cm^{-2}, the voltage decreased dramatically at a very low current density, reaching −1.0 V at 0.1 mA cm^{-2}. Different voltage values in the low current density region in the presence and absence of O_2 in the electrolyte indicates that the ORR is certainly involved in the cathodic reaction during the discharging process.

Cyclic voltammetry measurements were performed in both O_2- and N_2-saturated PBS solutions to evaluate the reactions at the Ti/TiO_2/Au cathode at 37 °C (Figure 2a). Under O_2-saturated conditions, the reduction and oxidation peaks for Ti/TiO_2/Au appeared around −0.3 V and 0.1 V vs. Ag/AgCl, respectively, whereas negligible current was observed in this voltage range under N_2-saturated conditions. These different electrochemical behaviors, which depend on the presence of O_2 in the electrolyte, clearly confirm that an ORR occurs in Ti/TiO_2/Au.

To determine whether the ORR proceeded through a two-electron or four-electron pathway, we first measured the amount of H_2O_2 produced during bulk electrolysis at an applied voltage of −0.4 V vs. Ag/AgCl (Figure 2b). Using the *N*,*N*-diethyl-*p*-phenylenediamine (DPD)/horseradish peroxidase (POD) method,[19] we calculated the Faradaic efficiency of H_2O_2 generation based on the measured H_2O_2 amount and the total charge transferred during bulk electrolysis at specific time points.[11] After 5 min of bulk electrolysis, the Faradaic efficiency was measured to be 65 %; it decreased slightly with time, reaching 40 % after 60 min of bulk electrolysis. The overall drop in Faradaic efficiency may be a result of further H_2O_2 reduction into H_2O.[11]

The reduction process at the Ti/TiO_2/Au cathode was further investigated using rotating-disk electrode (RDE) analysis in O_2-saturated PBS at 37 °C (Figure 2c,d). The electron transfer number (*n*), calculated from the slopes of the Koutecky–Levich plots,[11,20] was less than three from −0.40 V to −0.60 V vs. Ag/AgCl, suggesting that the two-electron process is more favorable than the four-electron process. In combination with the spectroscopic evidence for H_2O_2 generation, the formation of H_2O_2 through the ORR has thus been confirmed for our Mg-Ti/TiO_2/Au system. Additionally, rotating ring-disk electrode (RRDE) measurements also corroborate the generation of H_2O_2 through the ORR in both PBS and EBM-2 (endothelial growth basal medium; Figure S9).

Moreover, by using a metal conduit as a simple electric connection between the Mg anode and the Ti/TiO_2/Au cathode, H_2O_2 was generated in the absence of any applied external voltage or current in EBM-2 and PBS (Figure S10); a system without a metal connection (disconnected system) was used as the control. The amount of H_2O_2 formed in EBM-2 gradually increased over time for the connected system, reaching 16 μM after 30 min of connection whereas the amount of H_2O_2 was negligible (< 5 μM) for the disconnected system (Figure 3a). While negligible, the small amount of H_2O_2 generated in the control group may be a result of spontaneous Mg corrosion, which could generate H_2O_2 near the Mg surface.[21] A similar trend in H_2O_2 generation was observed for samples in PBS, although comparatively larger amounts of H_2O_2 were formed (ca. 50 μM) compared to those in EBM-2 (Figure 3b). This result is in good agreement with the RRDE result, which showed that both the ring currents and the H_2O_2 efficiencies are higher in PBS than in EBM-2 at the same applied voltage. Such differences in the H_2O_2 concentration might result from the different chemical compositions of PBS and EBM-2, which can influence the corrosion rate of magnesium.[22]

Based on previous reports, which showed that low levels of H_2O_2 can promote angiogenesis,[9,23] we investigated the effectiveness of our system for applications in vascular morphogenesis. An electrically connected Mg-Ti/TiO_2/Au system was introduced into EBM-2 media containing human umbilical vein endothelia cells (HUVECs CC-2517, Lonza; Figure 3c), and the amount of released H_2O_2 was controlled by changing the incubation time of the system. After incubation, the Mg-Ti/TiO_2/Au system was removed, and the culture medium was replaced with fresh culture medium without H_2O_2. The H_2O_2-stimulated HUVECs were then placed onto 96 well plates coated with Matrigel devoid of supplemental growth factors and cultured in EBM-2 media without supplemental growth factors. HUVECs without H_2O_2 stimulation cultured in EBM-2

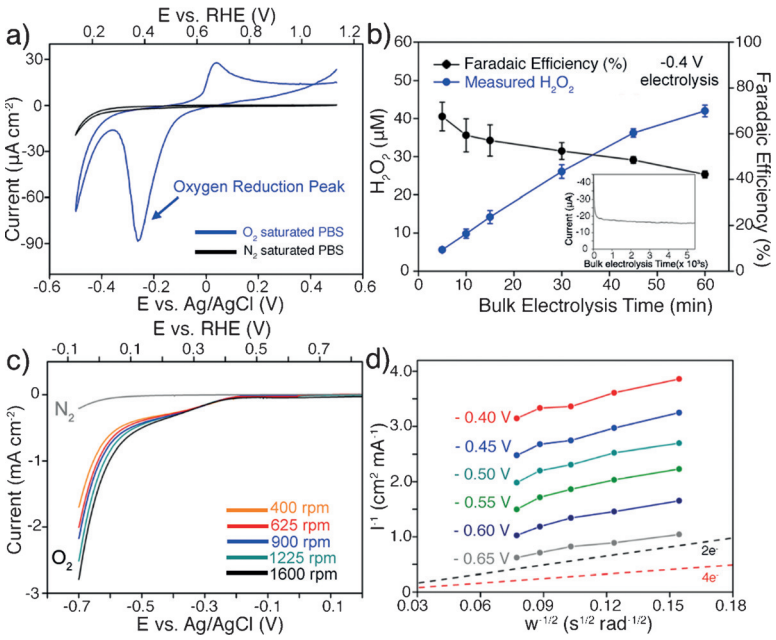

Figure 2. a) Cyclic voltammetry curves for the Ti cathode in O_2-saturated (blue) and N_2-saturated (black) PBS buffer. b) H_2O_2 concentration and Faradaic efficiency of H_2O_2 generation from the Ti/TiO_2/Au plate as a function of the bulk electrolysis time at an applied voltage of −0.4 V vs. Ag/AgCl. A bulk electrolysis profile is shown in the inset. c) Linear sweep voltammetry curves for the Ti/TiO_2/Au plate with various rotation rates in O_2-saturated PBS buffer. The background curve was obtained in N_2-saturated PBS buffer (gray). d) Koutecky–Levich plots for the Ti/TiO_2/Au plate as a function of the applied voltage; *n* values: 2.4 (R^2 = 0.98, −0.40 V), 2.3 (R^2 = 0.99, −0.45 V), 2.5 (R^2 = 0.96, −0.50 V), 2.4 (R^2 = 0.96, −0.55 V), 2.8 (R^2 = 0.97, −0.60 V), and 3.8 (R^2 = 0.98, −0.65 V).

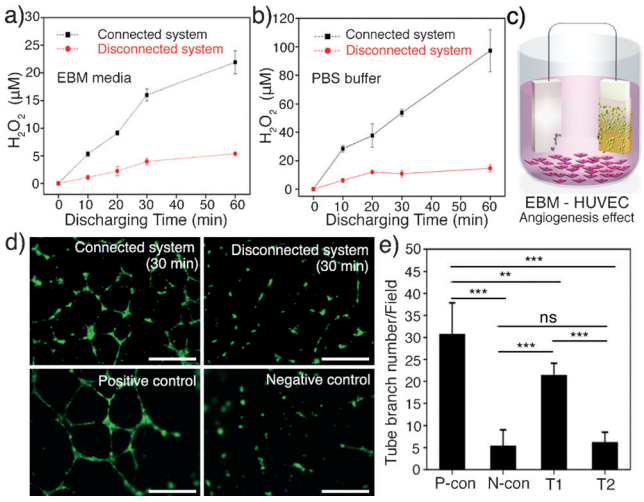

Figure 3. a) Concentration of H_2O_2 generated from connected (black) and disconnected (red) Mg-Ti/TiO_2/Au cells in a) EBM-2 medium and b) PBS buffer. c) Experimental setup for determining the effect of the Mg-Ti/TiO_2/Au system on vascular morphogenesis. d) Representative images of HUVEC tube formation on Matrigel after culturing in a connected system for 30 min or in a disconnected system for 30 min and the positive and negative controls (scale bar: 500 μm). e) Pooled data from five independent experiments, showing the total number of tube branches per field; the area of a single field is 2.35 mm^2. The T1 and T2 groups are HUVECs that were cultivated in a connected system or in a disconnected system, respectively, for 30 min.

media with or without supplementary growth factors were chosen as positive and negative control groups, respectively.

Interestingly, after 8 h of cultivation, HUVECs incubated for 30 min in a connected system showed capillary formation (Figure 3d). On the other hand, HUVECs incubated for 30 min in the disconnected system exhibited negligible capillary formation; this result was similar to that of the negative control (Figure 3d). Quantitative analysis showed that the average number of tube branches per field is approximately 23 for HUVECs pre-stimulated in a connected system, but below 5 for those stimulated in a disconnected system (Figure 3e). Whereas the positive control group showed a higher number of tube branches, the distinct difference compared to the other control groups is worthwhile to be noticed.

These results are in line with a previous report, which had described that 10 μM of H_2O_2, which is similar to the concentration range of our connected system when incubated for 30 min, facilitates vascular morphogenesis.[23] Moreover, quantification of the DNA content with a PicoGreen assay demonstrated an enhanced number of HUVECs in the connected system compared to that of the negative control group and the disconnected system (Figure S11). Put together, we have demonstrated that our system can be used to promote angiogenesis by the spontaneous generation of H_2O_2.

It should be noted that contrary to the positive results observed at low levels of H_2O_2 stimulation, in HUVECs exposed to high levels of H_2O_2 (approximately 100 μM for 30 min) angiogenesis is not promoted; instead, the cell number is reduced because of the oxidative stress induced by H_2O_2 (Figure S12).[2,23] Interestingly, the high levels of H_2O_2 generated using the connected system had an antibacterial effect as observed with *E. coli* suspended in PBS (Figure S13). These results highlight the importance of the controlled generation of H_2O_2 for promoting angiogenesis and simultaneously draw our attention to another potential use of our system, namely as an antibacterial agent. The release of H_2O_2 can be controlled by carefully adjusting the discharging time or other process parameters, such as the anodizing potential, to render our system suitable for further biological applications (Figure S14).

Finally, based on the effect of our Mg-Ti/TiO_2/Au system on angiogenesis, we designed a new Ti-based implant prototype by physically integrating Mg inside a screw-type Ti implant. Owing to the metallic nature of Mg and Ti, electrons generated from the corrosion reaction of Mg can easily be transferred to the Ti surface through the Mg/Ti interface without any supporting conductors. The integrated prototype after surface oxidation and gold deposition was then employed in EBM-2 media containing HUVECs (Figures 4 and S15). An enhanced level of HUVEC tube formation was observed compared to that of the negative control, and 15 min of incubation time gave the optimum effect for vascular morphogenesis (Figures 4c and S15). This result suggests that

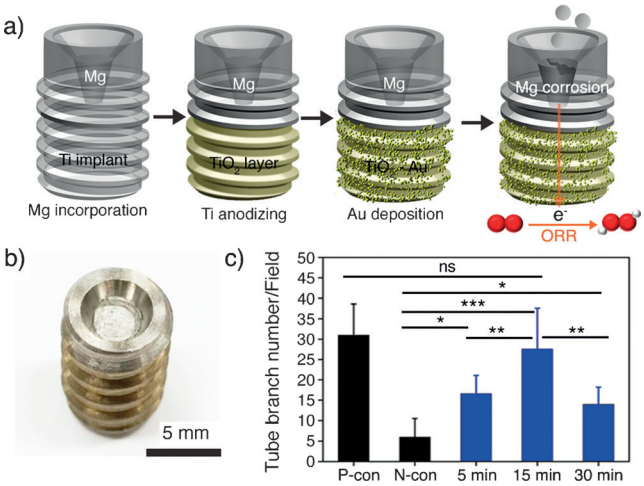

Figure 4. a) Fabrication of an integrated Mg-Ti/TiO_2/Au implant prototype. The Mg anode was incorporated into the Ti implant maintaining the metal contact, followed by Ti implant anodization and Au sputtering. Using the electrons generated from the corrosion of Mg, the ORR spontaneously occurs at the surface of the Ti implant. b) Optical image of the integrated prototype. c) The total number of tube branches per field depends on how long the HUVECs are exposed to the implant prototype, as assessed in five independent experiments.

conventional Ti orthopedic implants can be improved to support angiogenesis by the simple integration of Mg inside the implants.

In summary, we have designed a novel metal-based electrochemical system that spontaneously produces H_2O_2 by coupling biocompatible magnesium and oxidized titanium. Mg corrosion induces the transfer of electrons from Mg to TiO_2, which in turn generates H_2O_2 in the absence of an

external potential source. By controlling the amount of H_2O_2 released by varying the discharging time, we demonstrated that our system can be used for promoting angiogenesis. Moreover, we incorporated Mg into conventional Ti implants to achieve an enhanced level of angiogenesis, and showcased the potential application of the Mg/Ti integrated system as a functional orthopedic implant. We envision that our approach of utilizing the corrosion of biocompatible metals to generate electrons can be further extended to triggering other redox reactions in biological systems.

Acknowledgements

This research was supported by KIST (2E25260, 2E25122). We thank Dr. Thomas J. Meyer and Dr. Matthew Sheridan at the University of North Carolina at Chapel Hill for helpful comments.

Keywords: angiogenesis · catalysis · corrosion · magnesium · oxygen reduction reaction

How to cite: *Angew. Chem. Int. Ed.* **2015**, *54*, 14753–14757
Angew. Chem. **2015**, *127*, 14966–14970

[1] B. C. Dickinson, C. J. Chang, *Nat. Chem. Biol.* **2011**, *7*, 504–511.
[2] S. G. Rhee, *Science* **2006**, *312*, 1882–1883.
[3] C. C. Winterbourn, *Nat. Chem. Biol.* **2008**, *4*, 278–286.
[4] H. F. Krug, P. Wick, *Angew. Chem. Int. Ed.* **2011**, *50*, 1260–1278; *Angew. Chem.* **2011**, *123*, 1294–1314.
[5] C. R. Patra, J.-H. Kim, K. Pramanik, L. V. d'Uscio, S. Patra, K. Pal, R. Ramchandran, M. S. Strano, D. Mukhopadhyay, *Nano Lett.* **2011**, *11*, 4932–4938.
[6] W. He, H.-K. Kim, W. G. Wamer, D. Melka, J. H. Callahan, J.-J. Yin, *J. Am. Chem. Soc.* **2014**, *136*, 750–757.
[7] R. Cai, Y. Kubota, T. Shuin, H. Sakai, K. Hashimoto, A. Fujishima, *Cancer Res.* **1992**, *52*, 2346–2348.
[8] P. D. Ray, B.-W. Huang, Y. Tsuji, *Cell. Signalling* **2012**, *24*, 981–990.
[9] C. Xia, Q. Meng, L.-Z. Liu, Y. Rojanasakul, X.-R. Wang, B.-H. Jiang, *Cancer Res.* **2007**, *67*, 10823–10830.
[10] J. Macak, F. Schmidt-Stein, P. Schmuki, *Electrochem. Commun.* **2007**, *9*, 1783–1787.
[11] H. Sheng, H. Ji, W. Ma, C. Chen, J. Zhao, *Angew. Chem. Int. Ed.* **2013**, *52*, 9686–9690; *Angew. Chem.* **2013**, *125*, 9868–9872.
[12] S. V. Mentus, *Electrochim. Acta* **2004**, *50*, 27–32.
[13] H. Hermawan, D. Dubé, D. Mantovani, *Acta Biomater.* **2010**, *6*, 1693–1697.
[14] A. J. Bard, R. Parsons, J. Jordan, *Standard potentials in aqueous solution*, *Vol. 6*, CRC, New York, **1985**.
[15] P.-R. Cha, H.-S. Han, G.-F. Yang, Y.-C. Kim, K.-H. Hong, S.-C. Lee, J.-Y. Jung, J.-P. Ahn, Y.-Y. Kim, S.-Y. Cho, J. Y. Byun, K.-S. Lee, S.-J. Yang, H.-K. Seok, *Sci. Rep.* **2013**, *3*, 2367.
[16] M. Geetha, A. Singh, R. Asokamani, A. Gogia, *Prog. Mater. Sci.* **2009**, *54*, 397–425.
[17] A. Pérez del Pino, J. Fernández-Pradas, P. Serra, J. Morenza, *Surf. Coat. Technol.* **2004**, *187*, 106–112.
[18] L. Yin, X. Huang, H. Xu, Y. Zhang, J. Lam, J. Cheng, J. A. Rogers, *Adv. Mater.* **2014**, *26*, 3879–3884.
[19] H. Bader, V. Sturzenegger, J. Hoigné, *Water Res.* **1988**, *22*, 1109–1115.
[20] A. J. Bard, L. R. Faulkner, *Electrochemical Methods*, *2nd ed.*, Wiley, New York **2001**.
[21] J. R. Churchill, *Trans. Electrochem. Soc.* **1939**, *76*, 341–357.
[22] A. Yamamoto, S. Hiromoto, *Mater. Sci. Eng. C* **2009**, *29*, 1559–1568.
[23] M. Yasuda, Y. Ohzeki, S. Shimizu, S. Naito, A. Ohtsuru, T. Yamamoto, Y. Kuroiwa, *Life Sci.* **1998**, *64*, 249–258.

Received: August 7, 2015
Published online: October 20, 2015

